International Journal of Pharmaceutics 430 (2012) 307–317

Contents lists available at SciVerse ScienceDirect

International Journal of Pharmaceutics

journal homepage: www.elsevier.com/locate/ijpharm

Pharmaceutical Nanotechnology

Characterization, efficacy, pharmacokinetics, and biodistribution of 5 kDa mPEG modified tetrameric canine uricase variant

Chun Zhang[a], Kai Fan[b], Hua Luo[b], Xuefeng Ma[b], Riyong Liu[b], Li Yang[b], Chunlan Hu[b], Zhenmin Chen[b], Zhiqiang Min[b], Dongzhi Wei[a,*]

[a] State Key Laboratory of Bioreactor Engineering, Newworld Institute of Biotechnology, East China University of Science and Technology, Shanghai 200237, PR China
[b] Fagen Biomedical Inc., Chongqing 400041, PR China

ARTICLE INFO

Article history:
Received 9 February 2012
Received in revised form 17 March 2012
Accepted 31 March 2012
Available online 5 April 2012

Keywords:
PEGylated uricase
PEGylation homogeneity
Pharmacokinetics
Biodistribution
Elimination mechanism

ABSTRACT

PEGylated uricase is a promising anti-gout drug, but the only commercially marketed 10 kDa mPEG modified porcine-like uricase (Pegloticase) can only be used for intravenous infusion. In this study, tetrameric canine uricase variant was modified by covalent conjugation of all accessible ε amino sites of lysine residues with a smaller 5 kDa mPEG (mPEG-UHC). The average modification degree and PEGylation homogeneity were evaluated. Approximately 9.4 5 kDa mPEG chains were coupled to each monomeric uricase and the main conjugates contained 7–11 mPEG chains per subunit. mPEG-UHC showed significantly therapeutic or preventive effect on uric acid nephropathy and acute urate arthritis based on three different animal models. The clearance rate from an intravenous injection of mPEG-UHC varied significantly between species, at 2.61 mL/h/kg for rats and 0.21 mL/h/kg for monkeys. The long elimination half-life of mPEG-UHC in non-human primate (191.48 h, intravenous injection) indicated the long-term effects in humans. Moreover, the acceptable bioavailability of mPEG-UHC after subcutaneous administration in monkeys (94.21%) suggested that subcutaneous injection may be regarded as a candidate administration route in clinical trails. Non-specific tissue distribution was observed after administration of ^{125}I-labeled mPEG-UHC in rats, and elimination by the kidneys into the urine is the primary excretion route.

© 2012 Elsevier B.V. All rights reserved.

1. Introduction

Uricase (EC 1.7.3.3) is an enzyme involved in the purine degradation pathway and catalyzes the hydrolysis of uric acid to allantoin, which is readily excreted by the kidneys (Hediger et al., 2005). Humans lack active uricase because of gene mutations, leading to uric acid as the end product of purine metabolism (Christen et al., 1970) and resulting in the development of gout when the concentration of uric acid reaches its solubility limit in blood (hyperuricemia). A 10 kDa mPEG modified porcine-like recombinant uricase (Pegloticase) has been approved by the FDA on 14th September 2010 in treating severe tophaceous gout (Schlesinger et al., 2011), but the drug can only be injected intravenously (Biggers and Scheinfeld, 2008; Sherman et al., 2008), which may lower patient compliance during chronic therapy. Subcutaneous administration of Pegloticase was terminated in Phase I clinical study because of the slow release from the injection site and injection-site reactions (Sherman et al., 2008). Modification with smaller 5 kDa mPEG may accelerate the absorption from the injection site, relieve the injection-site reactions, and improve the bioavailability of subcutaneous administration. Therefore, 5 kDa mPEG, which has been used in the manufacture of several commercial pegylated proteins (Hershfield, 1998; Parkinson et al., 2003; Pasut et al., 2008), was selected for the modification of uricase in this study.

In the case of homo-tetrameric uricase, saturated pegylation using all accessible ε amino sites of lysine residues has been successfully developed to reduce its immunogenicity (Sherman et al., 2008). In our previous study, we constructed and characterized four canine–human chimeric uricases. Fortunately, both the enzymatic activity and stability of the finalized canine uricase variant (UHC) were improved compared to the original canine uricase (Zhang et al., 2012). The canine uricase variant was then extensively modified with 5 kDa mPEG-SPA (mPEG-UHC). Low enzymatic retention was the largest obstacle in developing a 5 kDa PEG modified uricase (Chen et al., 1981; Schiavon et al., 2000). The enzymatic retention of 5 kDa mPEG-SPA modified canine uricase was improved to higher

Abbreviations: AUC, area under curve; BSA, bovine serum albumin; LS, light scattering; RI, refractive index; mPEG-SPA, mPEG-succinimidyl propionate; mPEG-UHC, 5 kDa mPEG modified recombinant canine uricase variant; MSU, monosodium urate; RP-HPLC, reverse phase-high performance liquid chromatograph; rIL-2, recombinant interleukin-2; SD rats, Sprague-Dawley rats; SE-HPLC, size exclusion-high performance liquid chromatograph; sTNF-RI, soluble tumor necrosis factor receptor type I; TCA, trichloroacetic acid; UA, uric acid; UHC, recombinant canine uricase variant.

* Corresponding author. Tel.: +86 21 64252981; fax: +86 21 64250068.
E-mail address: dzhwei@ecust.edu.cn (D. Wei).

0378-5173/$ – see front matter © 2012 Elsevier B.V. All rights reserved.
http://dx.doi.org/10.1016/j.ijpharm.2012.03.057

than 85% and its immunogenicity in vivo was significantly reduced by removing uricase aggregates and PEG diol containments (Zhang et al., 2012). Further investigations of the effect of 5 kDa mPEG modification on the efficacy, pharmacokinetics, biodistribution and elimination mechanism of the tetrameric canine uricase variant are required.

In this study, further characterizations of mPEG-UHC were performed using reverse phase high performance liquid chromatograph (RP-HPLC), size exclusion-HPLC (SE-HPLC), mass spectrometry and gradient gel electrophoresis. Targeted deletion of the uricase gene in mice has been used to evaluate the efficacy of uricase (Kelly et al., 2001) but this is difficult to replicate. Moreover, the well-established uricase inhibitor induced hyperuricemia animal models (Stavric et al., 1969) are unsuitable to evaluate the efficacy of uricase, due to their inhibition of enzymatic activity. No versatile animal model had been found to be suitable for evaluating the efficacy of therapeutic uricase on uric acid nephropathy and gouty arthritis. In this study, three different animal models were set up to evaluate, respectively, the urate-lowering efficacy, preventive effect on uric acid nephropathy and therapeutic effect on gouty arthritis. The pharmacokinetic properties and the bioavailability after subcutaneous injection of mPEG-UHC were evaluated in rodents and non-human primates by bioassay method. Native uricase is mainly eliminated by the hepatic route (Fujita et al., 1991) but it is known that PEG modification can prevent tissue distribution and protect from proteolytic and other degradation (Kang et al., 2009), which may affect its excretion mechanisms. The influences or improvements after 5 kDa mPEG modification of UHC on tissue distribution and the excretion mechanism were investigated by administration of ^{125}I-labeled mPEG-UHC in rats.

2. Materials and methods

2.1. Animals

Sprague-Dawley (SD) rats and Japanese white rabbits were obtained from Shanghai B&K Laboratory Animal Co., Ltd. Crab-eating macaques were from Suzhou Xishan Zhongke Laboratory Animal Co., Ltd. Chicken were obtained from Deyang Wenshi Animal Co., Ltd. All the animals were pathogen free and allowed to access food and water freely. The experiments were carried out in compliance with the National Institute of Health Guide for the Care and Use of Laboratory Animals.

2.2. Preparation of mPEG-UHC

Briefly, overlap extension PCR (Ho et al., 1989) was employed to generate the canine uricase variant gene based on the synthesized *Escherichia coli* codon-optimized canine uricase gene (Safra et al., 2005; Zhang et al., 2012). Recombinant UHC was expressed in *E. coli* and purified by ion exchange chromatography and size exclusion chromatography to remove impurities and large aggregates. 5 kDa mPEG-SPA (with less than 0.2% PEG diol) was obtained from Jenkem Co., Ltd. Purified tetrameric UHC was reacted with 5 kDa mPEG-SPA in sodium carbonate buffer (100 mM, pH 10.0) at 4 °C for 12 h. 5 kDa mPEG-SPA (an amount in 4-fold molar excess of total lysines present in uricase) dissolved in 10 mM HCl was added to the cold solution of uricase (4 mg/mL). The conjugation solutions were loaded on Sephacryl S 300 size exclusion column to remove by-products of PEGylation reactions. The purified mPEG-UHC solution was filtrated through 0.2 μm Mustang™E Membrane to remove bacteria and endotoxin.

2.3. Characterization of mPEG-UHC

The purity of mPEG-UHC was determined by analytical RP-HPLC and SE-HPLC. RP-HPLC was performed using a Waters Symmetry 300TM C_4 analytical column (4.6 mm × 150 mm, 5 μm) with a 30-min 5–95% linear gradient of acetonitrile, 0.1% trifluoroacetic acid, at a flow rate of 1 mL/min. SE-HPLC was performed on a Superose-6 10/300 GL column (Amersham Biosciences) using PBS, pH 7.4 as mobile phase. The sample was eluted at a flow rate of 0.4 mL/min and detected at 214 nm using an Agilent 1100 system. The enzymatic activity was measured by the decrease in absorbance at 293 nm due to enzymatic oxidation of uric acid using RP-HPLC (Conley and Priest, 1980; Greenberg and Hershfield, 1989). The average degree of modification in the mPEG-UHC was evaluated by determining the average molecular weight of both the tetrameric protein moiety and the whole PEGylated tetrameric protein using SE-HPLC with online light scattering (LS), refractive index (RI), and UV detection as described previously (Kendrick et al., 2001; Li et al., 2005). The instrument calibration constants K_{RI}/K_{LS} and K_{UV}/K_{RI} were determined with a standard protein (BSA). The pegylation homogeneity was analyzed by determining the molecular weight distribution of monomeric mPEG-UHC using mass spectrometry and gradient gel electrophoresis. PEGylated uricase reference standards with different coupled PEG chains were prepared by mixing appropriate amounts of PEGylated uricase that modified at a PEG/protein ratio of 1:1 (w/w) with PEGylated uricase that modified at a ratio of 16:1. Mass spectrometry was performed on a Bruker Autoflex II MALDI-TOF mass spectrometer, which utilized a solid-state laser (Nd:YAG, 355 nm), used sinapinic acid (SA) as matrix, and operated in linear, positive ion mode with a static accelerating voltage of 20 kV. SDS gradient gel electrophoresis was performed on NuPAGE Novex 3–8% Bis–Tris gels and stained with Coomassie blue R-250.

^{125}I-labeled mPEG-UHC, specific activity 100 μCi/mg, was radiolabeled by China Institute of Atomic Energy and purified by size-exclusion chromatography. It showed a radiochemical purity of 95.8%, as determined by chromatography using a γ-counter.

2.4. In vivo efficacy evaluations

2.4.1. Urate-lowering efficacy in normal chicken

In vivo urate-lowering efficacy of mPEG-UHC was evaluated using normal chicken, due to its lose of uricase activity and relatively higher levels of serum uric acid (Keebaugh and Thomas, 2010). 12-Week-old chicken (50% male and 50% female) were randomly divided into 5 groups (n = 8): (1) normal control group, (2) UHC group (1.0 mg/kg), (3) mPEG-UHC group (0.5 mg/kg), (4) mPEG-UHC group (1.0 mg/kg), (5) mPEG-UHC group (2.0 mg/kg). The control saline or drugs were injected via auricular vein. The blood was collected from wing vein at 24 h, 72 h, 120 h, 144 h, 168 h, 216 h. Ex vivo degradation of uric acid was prevented by rapid mixing of blood with an equal volume of 2 N perchloric acid on ice (Kelly et al., 2001). The supernatant was obtained by centrifugation at 10,000 rpm for 10 min and the uric acid concentration in the supernatant was determined at 293 nm using RP-HPLC (Greenberg and Hershfield, 1989).

2.4.2. Therapeutic effect on knee joint urate arthritis in rabbits

To evaluate the therapeutic effect of mPEG-UHC on gouty arthritis, knee joint urate arthritis model was set up by using Japanese white rabbits. Adult male rabbits (2.2–2.5 kg) were randomly divided into 5 groups (n = 6): (1) normal control group, (2) model group, (3) mPEG-UHC group (0.5 mg/kg), (4) mPEG-UHC group (1.0 mg/kg), (5) mPEG-UHC group (2.0 mg/kg). Monosodium urate (MSU) crystals (Coderre and Wall, 1988) (30 mg) suspended in 0.3 mL PBS or PBS control were injected intra-articularly into the left knee joint of rabbits. The control saline or drugs were administrated via auricular vein at the same time. The perimeter of the knee joints was measured at 0 h, 3 h, 6 h, 12 h, 24 h, 48 h and 72 h. Knee swelling degree was expressed as the

change in knee perimeter before and following the induction of inflammation (Ekundi-Valentim et al., 2010). The swelling inhibition rates (%) were calculated by the following formula: $((AUC_{model} - AUC_{treated})/AUC_{model}) \times 100$, where the AUC was the area under curve calculated from the swelling degree–time profiles (Edwards, 1999). All the rabbits were anesthetized at 72 h and their left knee synovial tissues were collected to make the histological section. The assessment of the histological acute joint inflammatory scores was performed using semiquantitative grading scales (Roth et al., 2005).

2.4.3. Preventive effect on uric acid nephropathy in rats

To evaluate the preventive effect of mPEG-UHC on uric acid nephropathy, acute uric acid nephropathy model in SD rats was induced by feeding yeast extract and injection of MSU crystals. Adult male rats (180–220 g) were randomly divided into 5 groups ($n = 6$): (1) blank control group, (2) model control group, (3) mPEG-UHC group (0.5 mg/kg), (4) mPEG-UHC group (1.0 mg/kg), (5) mPEG-UHC group (2.0 mg/kg). The control saline or drugs were administrated via tail vein at 0 d, 7 d, 14 d, 21 d, and 28 d. During this period, normal control group was fed with normal diet. Model and therapeutic groups were fed with the diet containing 10% yeast extract and injected intra-peritoneally with MSU suspended liquid (500 mg/kg) daily. The blood samples were collected from eyeground venous plexus at 27 d and 29 d to evaluate the urate level. All the rats were exsanguinated under anesthesia (urethane, 1.2 g/kg, intra-peritoneal injection) at 29 d, the blood was collected to test the creatinine and urea nitrogen concentration. The left renal was collected to make histological section and evaluate the renal histopathological score (Monrad et al., 2008).

2.5. Bioavailability and pharmacokinetics studies

SD rats (180–220 g) and crab-eating macaques (3.5–4.0 kg) were used to examine the bioavailability and pharmacokinetics of mPEG-UHC. SD rats (50% male and 50% female) were randomly divided into two groups ($n = 18$), which were treated with single intravenous or subcutaneous injection of mPEG-UHC (0.9 mg/kg). The blood samples were collected from the plexus venous in the eyeground at 1 h, 4 h, 6 h, 8 h, 12 h, 16 h, 24 h, 30 h, 36 h, 48 h, 60 h, 72 h, 96 h, 120 h and 144 h (six rats for each time point). Crab-eating macaques (50% male and 50% female) were randomly divided into two groups ($n = 6$), and treated with single intravenous or subcutaneous administration of mPEG-UHC (1.0 mg/kg). The blood samples were collected from the upper limb vein at 0.03 h, 1 h, 6 h, 12 h, 24 h, 48 h, 72 h, 144 h, 192 h, 240 h, 288 h, 360 h, 432 h and 504 h. The mPEG-UHC concentrations were determined by evaluating the retention plasma enzymatic activity as described above. Drug and Statistics for Windows (DAS ver 2.0) was used to analyze the standard pharmacokinetic parameters. Elimination half life ($t_{1/2z}$), apparent volume of distribution (V_z), total body clearance rate (CL_z), area under concentration–time curve ($AUC_{0-\infty}$) and absolute bioavailability were calculated in a non compartmental manner based on the statistical moment theory.

2.6. Biodistribution and excretion studies

SD rats (180–220 g) were used to evaluate the biodistribution and excretion properties of mPEG-UHC. 24 SD rats (50% male and 50% female) were subcutaneous injected with ^{125}I-labeled mPEG-UHC (0.9 mg/kg). Rats were exsanguinated through femoral artery under anesthesia (urethane, 1.2 g/kg, intra-peritoneal injection) at 6 h, 16 h, 30 h, and 48 h after injection (six rats for each time point). The blood, brain, heart, lung, liver, spleen, kidney, stomach, intestine, muscle, and genital were collected. The serum and homogenized tissue solutions were prepared by diluting the weighted serum or tissue five times with 0.9% chloride solution and their total radioactivity was evaluated by a γ-counter without any special procedure. The TCA-precipitable radioactivity was also measured. To 100 μL of serum or tissue solution, 100 μL of 20% TCA was added (Liu et al., 2005). The mixture was vortexed for 2 min, and the supernatant was removed. The radioactivity of the precipitate was determined by a γ-counter.

For excretion studies, SD rats (50% male and 50% female) were randomly divided into two groups ($n = 6$). Both groups were subcutaneously injected with ^{125}I-labeled mPEG-UHC (0.9 mg/kg). Each rat in group one was placed in a separate glass metabolic cage. The urine and feces samples were collected at the fixed time intervals from 0 to 4 h, 4 to 8 h, 8 to 12 h, 12 to 24 h, 24 to 36 h, 36 to 48 h, 48 to 60 h, 60 to 72 h, 72 to 96 h, 96 to 120 h, 120 to 144 h, 144 to 168 h and 168 to 192 h. The other group was used to determine the bile excretion. The rats in the group were anesthetized (urethane, 1.2 g/kg, intra-peritoneal injection) and operated by the bile duct-cannulation method. Then, the rats were injected as described above. The bile samples were collected at the fixed time intervals from 0 to 2 h, 2 to 4 h, 4 to 6 h, 6 to 8 h, 8 to 12 h and 12 to 24 h. The total volume of urine and bile was measured, and the feces was freeze-dried, weighted, and pulverized. The excretion amounts were determined by calculating the total radioactivity.

2.7. Statistical analysis

All results were expressed as the mean ± standard deviation (SD) unless otherwise noted. Statistical analysis was performed by Student's *t*-test for two groups, and one-way ANOVA for multiple groups. A probability (p) of less than 0.05 is considered statistically significant.

3. Results

3.1. Characterization of mPEG-UHC

The detailed PEGylation and purification results were shown in our previous study (Zhang et al., 2012). As shown in Fig. 1, the purity of mPEG-UHC was greater than 98% as judged by RP-HPLC and SE-HPLC after purification by Sephacryl S 300 size exclusion column and the resulting mPEG-UHC had a specific activity of 12 U/mg as determined at 37 °C, pH 8.6.

The average molecular weights of the tetrameric protein moiety and the whole tetrameric mPEG-UHC were 127.6 kDa and 323.5 kDa as determined by SE-HPLC LS–RI–UV system. The evaluated molecular weight of tetrameric UHC protein was essentially the same as that calculated by the amino acid sequence (137.0 kDa), indicating the accuracy of the above technique. As the literal molecular weight of a single 5-kDa mPEG chain is 5.2 kDa (calculated by MALDI-TOF, date not shown), the average 5 kDa mPEG chains that coupled to each uricase tetramer could be calculated by the following equation: $N = (323.5 - 127.6)/5.2 = 37.7$, which means that approximately 9.4 5 kDa mPEG chains were coupled to each uricase monomer.

The MALDI-TOF spectrum of PEGylated uricase reference standards is shown in Fig. 2A. The spectrum showed the presence of twelve peaks with m/z values of 34,272, 39,727, 44,923, 50,630, 56,040, 61,334, 66,947, 72,430, 77,904, 82,950, 87,750 and 93,283 Da, respectively. The molecular weigh of a UHC monomer is 34.2 kDa. Therefore, the peak designated "No PEG" may be considered to arise from native UHC monomer. Each of the adjacent peaks designated "1–11 PEG" is determined to be separated by approximately 5.2–5.4 kDa, which agrees with the average molecular

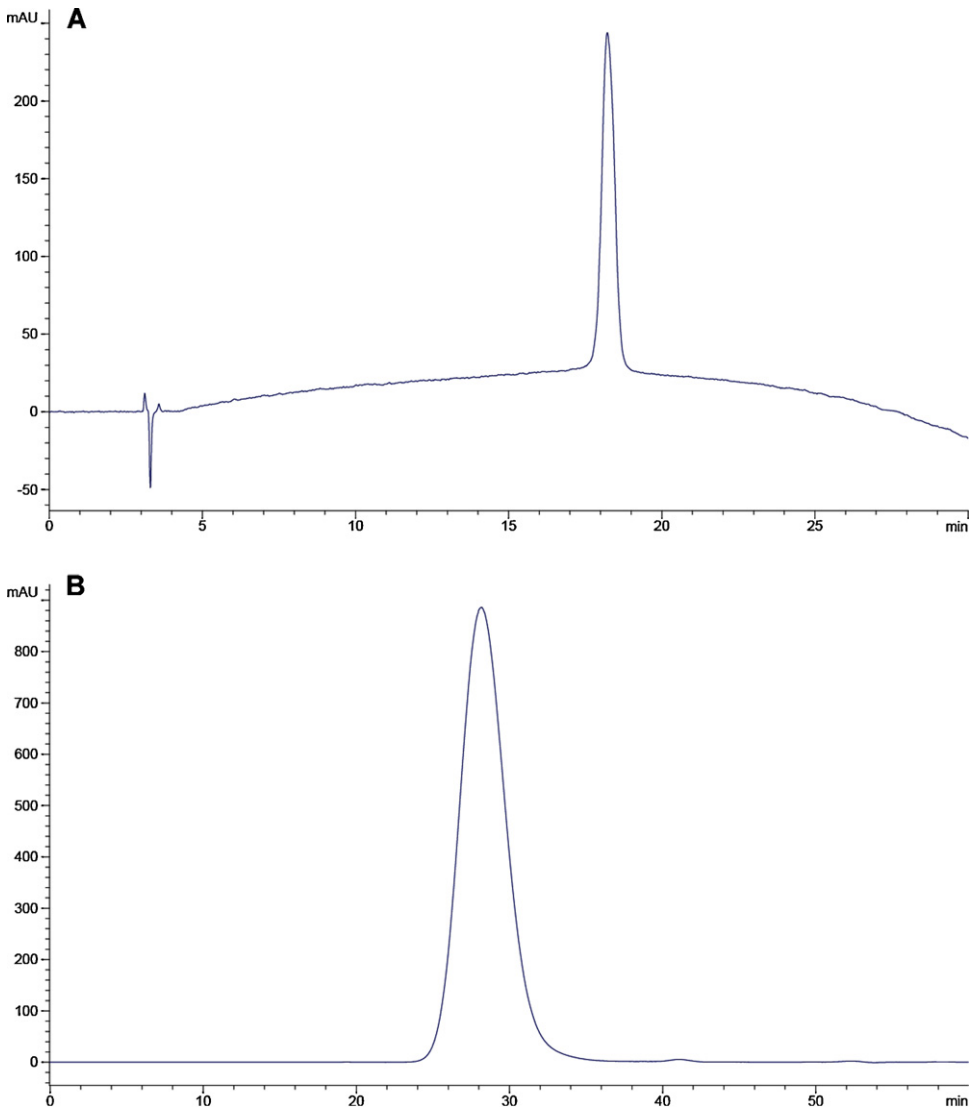

Fig. 1. RP-HPLC (A) and SE-HPLC (B) analyses of purified mPEG-UHC. Peaks were detected using a UV detector (Agilent 1100 system) set at 214 nm.

weigh of a single 5 kDa mPEG chain, indicating that the above peaks represent different species with the indicated number of PEG chains bound to UHC monomer. The MALDI-TOF spectrum of mPEG-UHC (Fig. 2B) showed the presence of five peaks with *m*/*z* values of 72,581, 77,818, 82,886, 87,528 and 93,303 Da, respectively, which represent monomeric mPEG-UHC with 7–11 coupled mPEG chains. The PEGylation homogeneity was also checked by gradient gel electrophoresis. As shown in Fig. 3, PEGylated uricase reference standards could also be separated to different protein bands. The lowest band ranged between 30 kDa and 40 kDa should be the native UHC monomer. According to the MALDI-TOF spectrum, the other PEGylated protein bands were designated. The molecular weights of other PEGylated protein bands are inconsistent with the standard protein markers, which may be caused by the interference of the coupled mPEG in protein mobility. The PEGylation homogeneity that was determined by SDS gradient gel electrophoresis agrees essentially with that evaluated by MALDI-TOF. No PEGylated uricase that coupled less than 6 mPEG chains per monomer was observed in denatured monomeric mPEG-UHC, but it is difficult to evaluate the exact number of coupled mPEG chains in mPEG-UHC due to the low-resolution of PEGylated uricases that coupled more than 7 mPEG chains per monomeric UHC in gel electrophoresis.

3.2. *In vivo efficacy assessment*

3.2.1. *Urate-lowering efficacy in normal chicken*

Birds, similar to humans, also excrete uric acid as the end product of purine metabolism because of the lack of active uricase in vivo, resulting in higher blood uric acid level than that in most experimental mammals. The urate-lowering efficacy of unmodified UHC and mPEG-UHC in a normal chicken is shown in Fig. 4, in which the serum uric acid levels were stable between 180 and 210 μM/L. The serum level of uric acid level could be lowered to 50 μM/L and maintained for 1, 3 and 5 d in low, median and high dose groups, respectively. In contrast, the uric acid level could only be decreased to 130 μM/L 24 h after injection with unmodified UHC.

3.2.2. *Therapeutic effect on knee joint urate arthritis in rabbits*

Gouty arthritis is a common symptom of hyperuricemia (Schlesinger, 2004), but, until now, only Coderre et al. had developed an ankle joint urate arthritis model in rats for the evaluation of anti-arthritic agents (Coderre and Wall, 1988). However, its versatile and diagnostic accuracy is low. In this study, a rabbit knee was used instead of a rat ankle to set up the joint urate arthritis models. As shown in Fig. 5, compared with normal rabbits, there

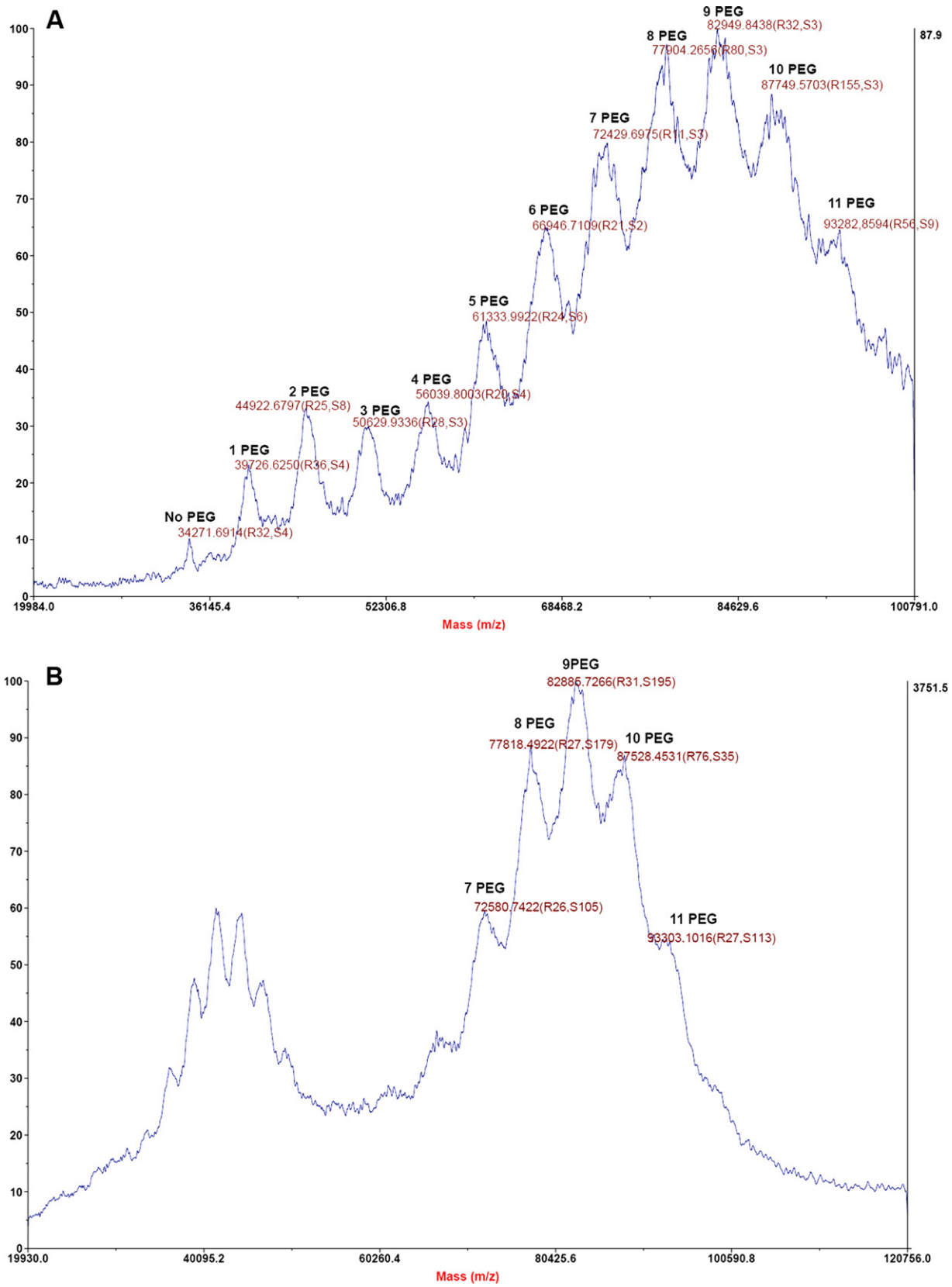

Fig. 2. MALDI-TOF spectrum of PEGylated uricase reference standards (A) and mPEG-UHC (B). The numbers on the peaks are the *m*/*z* values of the corresponding peaks. The markers designated "No PEG" and "1–11 PEG" indicate the number of PEG chains attached to monomeric UHC protein. Small double-charged mass (M^{2+}) peaks were also present in the spectrum of mPEG-UHC.

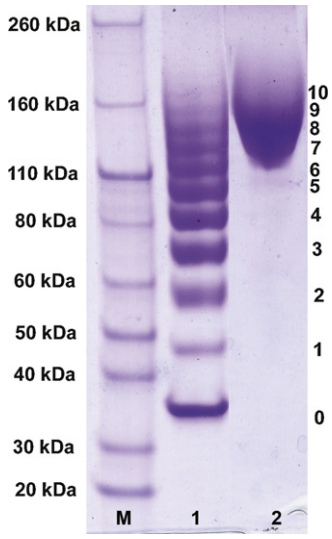

Fig. 3. SDS-PAGE analysis of PEGylated uricase reference standards and mPEG-UHC. Lanes: M, standard protein molecular weight markers; 1, PEGylated uricase reference standards; 2, mPEG-UHC. The numbers designated "0–10" indicate the number of PEG chains attached to monomeric UHC protein.

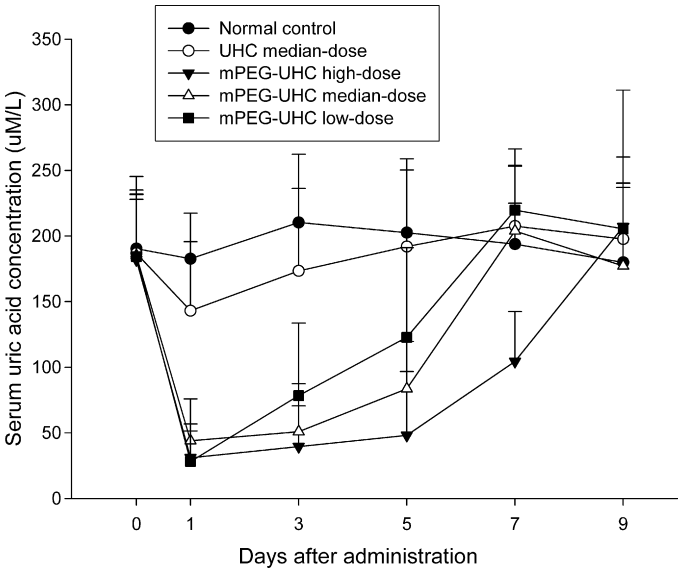

Fig. 4. Urate-lowering efficacy of mPEG-UHC in normal chicken. The serum uric acid concentration was determined at 293 nm using RP-HPLC.

was significant joint swelling in the model group 3 h after injection of MSU and the swelling degree increased up to 24 h and then continued to slowly decrease during the next 48 h. Administration of mPEG-UHC markedly inhibited the swelling degree from 3 h in a dose-dependent manner (Fig. 6). The swelling degree in all the mPEG-UHC treated groups could return to normal at 72 h, compared with that obtained from the normal control group. Moreover, the results of histological acute joint inflammatory scores showed that the scores at all three doses were slightly higher than those of normal rabbits and significantly lower than those of the model rabbits, indicating that mPEG-UHC could dissolve the MSU in the knee joint and inhibited the swelling and acute joint inflammation.

3.2.3. Preventive effect on uric acid nephropathy in rats

Uric acid nephropathy is another frequent symptom of hyperuricemia (Liebman et al., 2007). The blood uric acid level (50 μM/L) in rat is much lower than its saturated solubility under physiological conditions due to the existence of active uricase in the liver (Mazzali et al., 2001). In this study, intra-gastric administration of yeast extract or intra-peritoneal injection of high dose MSU (1000 mg/mL) was initially attempted but failed to build the uric acid nephropathy model because of high fatality. We finally achieved this by supplementing the diet with yeast extract and daily intra-peritoneal injections of a low dose of MSU, as described in Section 2. Blood biochemistry data (Table 1) showed that the serum uric acid level in model rats increased to 200 μM/L and could be maintained for over 4 weeks. In addition, both the creatinine level and the histopathological scores for the kidney in model rats were significantly higher than those in normal rats, suggesting that the uric acid nephropathy model was successfully attained. After weekly administration of mPEG-UHC, the serum uric acid concentrations were maintained below 30, 65, and 120 μM/L in the 2, 1, and 0.5 mg/kg dose groups, respectively. Moreover, the kidney histopathological scores showed that pretreatment with mPEG-UHC could prevent kidney histopathological injury in a dose-dependent manner and the blood creatinine levels in all mPEG-UHC-treated rats could be significantly reduced 4 weeks after injection. mPEG-UHC showed definitely preventative effects on uric acid nephropathy in rats.

3.3. Bioavailability and pharmacokinetics studies

The blood concentrations of mPEG-UHC were calculated by determining retention enzyme activity in plasma. Our unpublished documents showed that the elimination half-life after intravenous administration of unmodified UHC (1.0 mg/kg) in crab-eating macaques was only 1.29 h, while, after PEGylation such parameters increased dramatically. The pharmacokinetic parameters and concentration–time profiles of mPEG-UHC after single subcutaneous or intravenous administration in SD rats and crab-eating macaques are shown in Table 2 and Fig. 7. For SD rats, the elimination half lives, $t_{1/2z}$, for subcutaneous and intravenous administration were 28.39 and 32.32 h, respectively. Comparison of $AUC_{0-\infty}$ values between the intravenously and subcutaneously injected groups, indicated an absolute bioavailability of 58.57% for subcutaneous injection. For crab-eating macaques, the elimination half lives after subcutaneous and intravenous administration were 163.79 and 191.48 h, respectively, whereas the absolute bioavailability of subcutaneous injection was 94.21%. It is important to note that the clearance rate from an intravenous injection varied significantly between species, at 2.61 mL/h/kg for rats and 0.21 mL/h/kg for monkeys.

3.4. Biodistribution and excretion studies

The biodistribution characteristics of mPEG-UHC were determined at different time intervals by measuring the total and TCA-precipitable radioactivity, respectively. The distribution levels in all organs, especially in kidney, determined by total radioactivity were higher than those determined by TCA-precipitable radioactivity, which may be caused by the degradation of ^{125}I-labeled mPEG-UHC and dissociation of radioiodine from mPEG-UHC proteins in organs. The largest relative disparity occurred at 6 h due to the extra degradation during the subcutaneous absorption period. As shown in Fig. 8, mPEG-UHC showed a broad tissue distribution and the highest concentration of mPEG-UHC was found in the kidney, followed by lung and liver. The mPEG-UHC concentrations in brain and muscle were the lowest among all the organs examined. More importantly, the concentration of mPEG-UHC in blood was much higher than that in the organs, which indicated that most of the mPEG-UHC was retained in blood and little non-specific accumulation occurred in tissues.

Table 1
Preventive effect of mPEG-UHC on uric acid nephropathy in rats.

Items	UA (μM/L)		CRE (μM/L)	BUN (mM/L)	Histopathological score
	24 h before last administration	24 h after last administration			
Normal control	58.43 ± 5.31	66.47 ± 6.11	94.33 ± 10.75	9.10 ± 1.16	0.00 ± 0.00
Model control	199.70 ± 11.79	193.72 ± 31.13	125.15 ± 4.19	9.26 ± 1.57	4.71 ± 1.38
High-dose	16.77 ± 13.36***	0 ± 0***	96.12 ± 5.14***	8.47 ± 0.92	1.44 ± 1.33**
Median-dose	61.70 ± 15.31***	2.93 ± 2.43***	105.23 ± 7.38**	9.52 ± 1.75	1.67 ± 0.89**
Low-dose	116.59 ± 26.06***	8.17 ± 14.32***	108.22 ± 14.04*	9.71 ± 2.05	2.17 ± 1.17**

Date represent mean value ± SD.
* Significantly different from the model control at level of $p < 0.05$.
** Significantly different from the model control at level of $p < 0.01$.
*** Significantly different from the model control at level of $p < 0.001$.

Table 2
Pharmacokinetic parameters of mPEG-UHC after single subcutaneous or intravenous administration in rats and monkeys.

	Rats		Monkeys	
	Intravenous injection	Subcutaneous injection	Intravenous injection	Subcutaneous injection
T_{max} [a] (h)	1	16	0.03	56
$t_{1/2z}$ [b] (h)	32.32	28.39	191.48	163.79
V_z [c] (L/kg)	0.12	0.18	0.06	0.05
CL_z [d] (mL/h/kg)	2.61	4.46	0.21	0.23
$AUC_{0-\infty}$ [e] (mg h/L)	344.64	201.84	4998.09	4708.65
F [f] (%)	100	58.57	100	94.21

[a] Time to maximum concentration.
[b] Elimination half life.
[c] Apparent volume of distribution.
[d] Total body clearance rate.
[e] Area under concentration–time curve.
[f] Absolute bioavailability.

The cumulative excretion–time curves of urine, feces and bile, assayed by the radioactivity method, are shown in Fig. 9. The cumulative urinary and feces excretion percentages were 85.66 and 4.61% up to 192 h post injection, while the cumulative biliary excretion percentage was only 3.14% within 24 h. From the combined results of biodistribution and excretion, most of the mPEG-UHC is eliminated by the kidneys into the urine and little hepatic metabolism and biliary

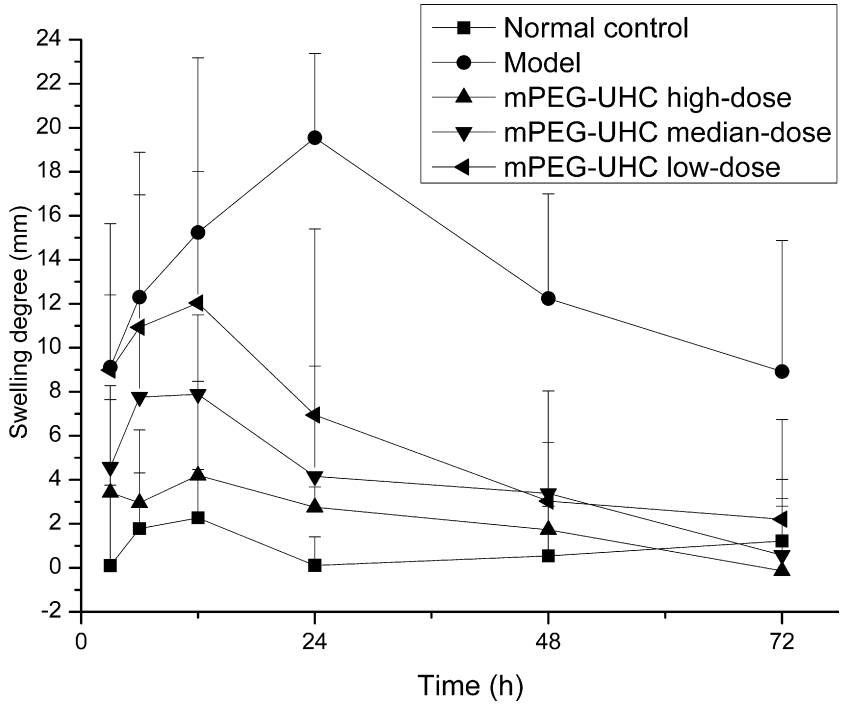

Fig. 5. Dose related inhibition of knee swelling by mPEG-UHC in MSU induced arthritis in rabbits. Knee swelling degree was expressed as the change in knee perimeter before and following the induction of inflammation.

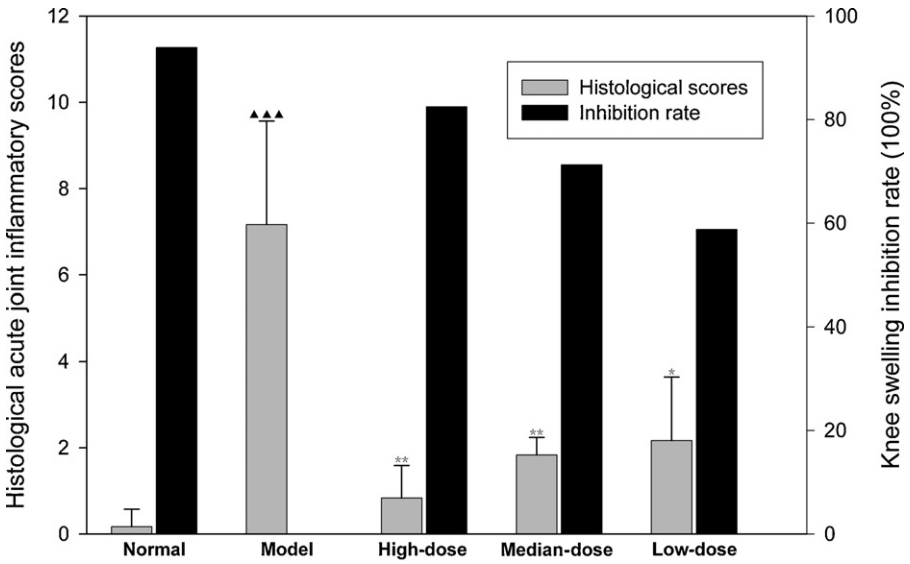

Fig. 6. Dose related histopathological score and inhibition rate of knee swelling by mPEG-UHC in MSU induced arthritis *, ** and *** mean significantly different from the model control at levels of $p < 0.05$, $p < 0.01$, and $p < 0.001$; ▲, ▲▲ and ▲▲▲ mean significantly different from the normal control at levels of $p < 0.05$, $p < 0.01$, and $p < 0.001$.

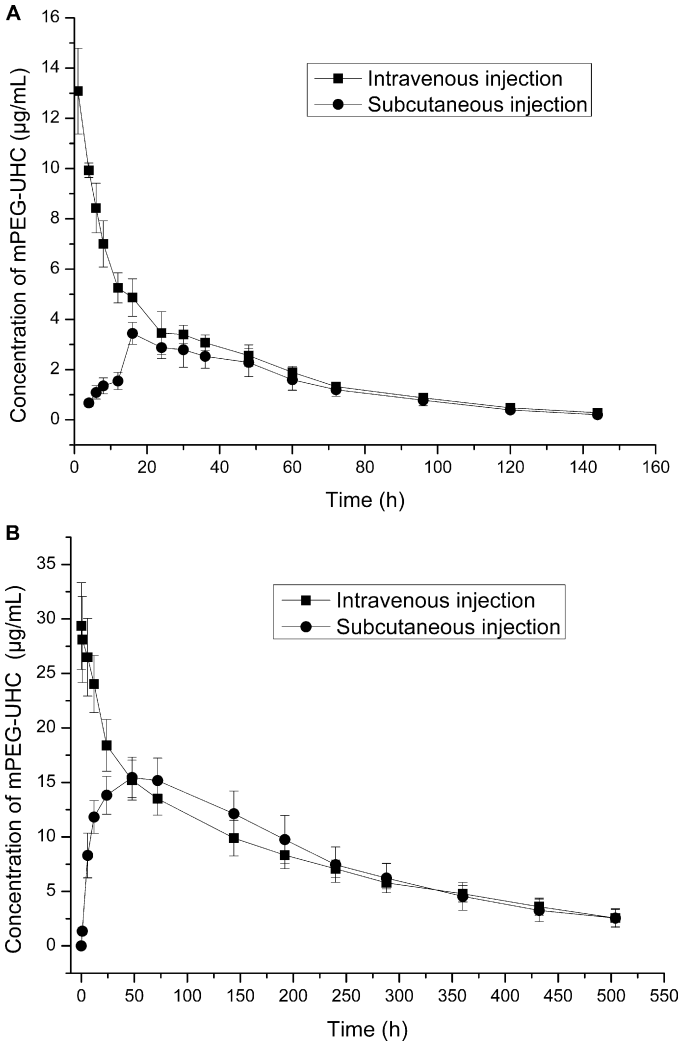

Fig. 7. Concentration–time curve of mPEG-UHC after single subcutaneous or intravenous administration in rats (A) and monkeys (B). The blood concentrations of mPEG-UHC were calculated by determining retention enzyme activity in plasma.

excretion was involved in the removal of the large PEGylated proteins.

4. Discussion

In our previous study, we constructed canine–human chimeric uricase with improved enzymatic characteristics compared to the original canine uricase (Zhang et al., 2012). Meanwhile, another study showed that unmodified uricase aggregates and cross-linked conjugates could trigger accelerated blood clearance. After removal of uricase aggregates and PEG diol contaminant, such behavior was successfully avoided (Zhang et al., 2012). In this study, the tetrameric canine uricase variant was modified by covalent conjugation of all accessible ε amino sites of lysine residues with 5 kDa mPEG.

Although one monomeric UHC protein contains 29 lysine residues, only 10–12 residues of each monomer would be accessible on the surface of the tetrameric enzyme (Caliceti et al., 2001; Sherman et al., 2008). In this study, the PEGylation homogeneity determined by gradient gel electrophoresis is essentially the same as that determined by mass spectrometry, which coincides well with the average modification degree determined by the SE-HPLC LS–RI–UV system. Approximately 9.4 mPEG chains were coupled to each UHC subunit after saturated modification with 5 kDa mPEG-SPA, which is consistent with the commercial pegylated porcine-like uricase (Pegloticase) that contains an average of 9 ± 1 strands of 10 kDa mPEG per subunit (Baraf et al., 2005; Sherman et al., 2008). It is known that the homogeneity of such nonspecific modification of multiple lysine residues is lower than other site-specific PEGylation (Roberts et al., 2002). The potential accessible lysines may be different among monomeric uricase due to the steric hindrance by the already conjugated PEG chains. Such interference may be increased in the case of extensively PEGylated tetrameric uricase. Moreover, the spatial structures of monomeric subunits are not exactly the same within the same tetramer (Retailleau et al., 2005), which may also cause the diversity of possible PEGylated sites among monomers and increase the heterogeneity of PEGylated subunits as determined by mass spectrometry and gradient gel electrophoresis. mPEG-UHC was stable when stored at 4 °C in neutral pH for one year under a relatively high concentration of 10 mg/mL and the resulting mPEG-UHC had

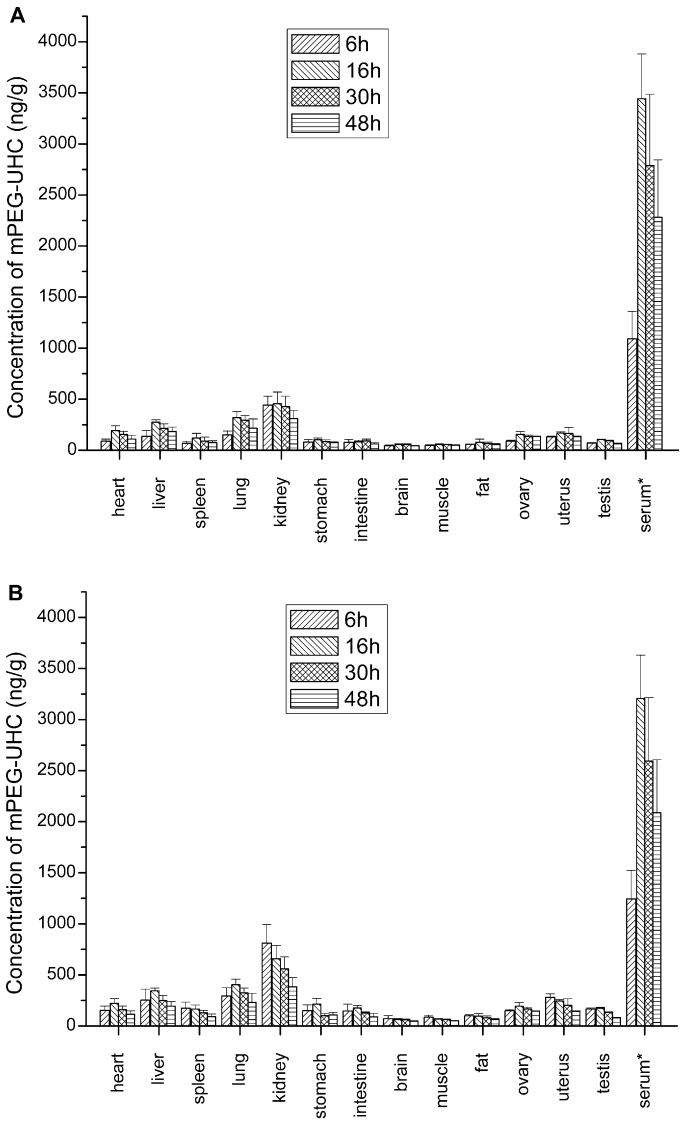

Fig. 8. Tissue distribution of ^{125}I-labeled mPEG-UHC in rats following subcutaneous administration. (A) and (B) were shown by measuring the TCA-precipitable and total radioactivity, respectively. *The serum concentration of mPEG-UHC was ng/mL.

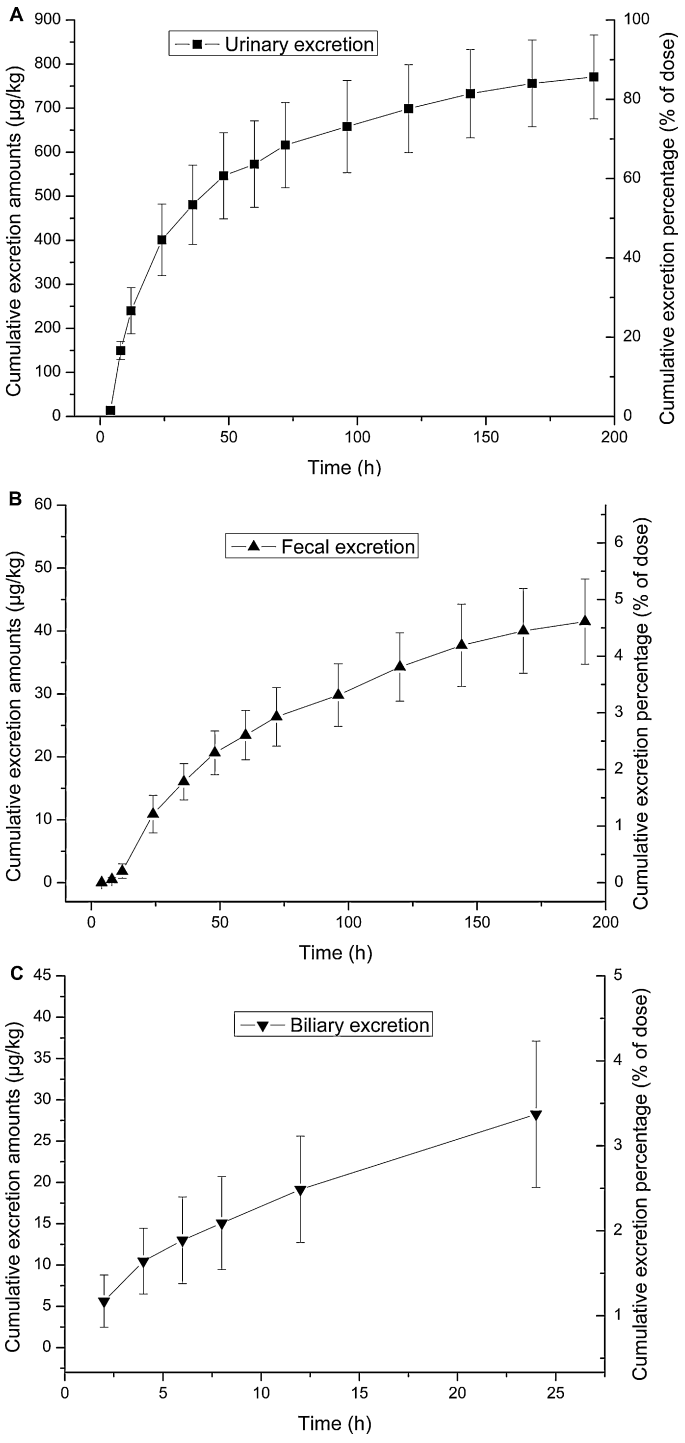

Fig. 9. Excretion curves after subcutaneous injection of ^{125}I-labeled mPEG-UHC in rats. (A) Excretion in urine. (B) Excretion in feces. (C) Excretion in bile.

a specific activity of 12 U/mg. These characteristics are important for further pharmacology evaluation.

The most frequent symptoms caused by hyperuricemia are uric acid nephropathy and gouty arthritis. In this study, we first set up a rat uric acid nephropathy model by supplementing the diet with yeast extract and daily intra-peritoneal injection of MSU. Weekly injections of mPEG-UHC could maintain low levels of uric acid and prevent pathological changes and functional lesions in kidneys. The urate arthritis model was built using a rabbit knee instead of rat ankle, which may improve diagnostic accuracy over ankle swelling. Administration of mPEG-UHC could quickly dissolve MSU in the knee joint and inhibit swelling within 72 h. In addition, according to urate-lowering efficacy of mPEG-UHC in normal chicken, single administration of mPEG-UHC with 9–18 IU/kg in the chicken could lower the blood uric acid level from 230 to 50 μM/L and maintain for 3–5 d, which coincides with the known effective human dose of 2.0–4.0 IU/kg (Sherman et al., 2008). Hence, we estimated 1.0 mg/kg as the preliminary biological effective dose for further work.

The pharmacokinetic profiles of mPEG-UHC varied strongly among different species, which is inconsistent with the results reported by Edwards et al., who pointed out that the plasma clearance of PEG sTNF-RI per body weight across the species was relatively constant (Edwards, 1999). Such differences may be due to their different sizes and elimination mechanisms. PEG sTNF-RI has a molecular weight of 42 kDa and may be filtered through the glomerulus (Edwards et al., 2003). In contrast, tetrameric mPEG-UHC greatly exceeds the glomerular filtration limit due to its high molecular weight (323.5 kDa). Knauf et al. reported that the systemic clearance of PEGylated rIL-2 was only slightly influenced by further increase of the conjugate size after its size reached the kidney ultrafiltration limit (Knauf et al., 1988). However, such profiles were obtained in the same animals and little is known about

the clearance rate of large conjugates among different species. In this study, the clearance rate of mPEG-UHC in monkeys was 10–20 times slower than that in rats. The biodistribution and excretion results showed that elimination by the kidneys into the urine is the primary route of excretion of mPEG-UHC in rats. Another mechanism of clearance may exist in monkeys, and result in the different clearance rates across species. If the elimination mechanism is the same within rats and monkeys, since PEGylated tetrameric uricase would exceed the renal filtration limit, while its main elimination is still through the renal route, the mostly likely clearance mechanism is that larger tetrameric conjugates were first depolymerized into monomers or degraded to low molecular mass segments during circulation and then filtered through the glomerulus and excreted with urine. The former step appears to be the limiting factor and may vary among different species, which may lead to the different clearance rates across species. On the contrary, small PEGylated proteins may directly filter through the glomerulus, resulting in a relatively consistent clearance among species, as described for PEG sTNF-RI (Edwards, 1999). Compared with rats, the elimination half-life after intravenous injection of mPEG-UHC in monkeys increased to 191.48 h, suggesting that the predicted elimination half-life in humans may also be longer than one week because of their high homology. Moreover, the systemic bioavailability of mPEG-UHC after subcutaneous administration in monkeys was higher than 90%, indicating that subcutaneous injection may be regarded as a candidate route for administration. Taken together, the elimination half-life of mPEG-UHC in humans may be the same as that of Pegloticase, but the former may accelerate the absorption from the injection site and improve the bioavailability of subcutaneous administration, which is important to develop more convenient administration routes and may enhance patient compliance during chronic therapy.

Caliceti et al. demonstrated that PEG molecular weight and structure could influence the tissue distribution of PEGylated uricase (Caliceti et al., 1999). The distribution levels in all organs were higher with fungal uricase modified with 10 kDa PEG than with 5 kDa PEG, meaning that smaller PEG moieties may prevent non-specific tissue distribution (Caliceti et al., 1999). According to the data in this study, little non-specific tissue distribution occurred, the highest concentration of mPEG-UHC was found in the kidney, which may contribute to the renal mediated elimination route. Moreover, the distribution level of mPEG-UHC in the spleen and liver was much lower than that of both 5 and 10 kDa modified fungal uricase (Caliceti et al., 1999), suggesting that little splenic or hepatic extraction occurred during the whole excretion process, together with the result that the amounts of mPEG-UHC that cleared through bile and feces were less than 10%. Saturated modification with smaller PEG not only masked the recognition site and charges of the protein but also diminished the distribution levels in all organs. In addition, removal of uricase aggregates before administration lowered the overall size of the PEG conjugates, which may help to avoid capture by the mononuclear phagocyte system in reticuloendothelial cell rich organs such as the liver and spleen. Based on the above effects, mPEG-UHC was apparently masked as stealth colloids and could reduce the tissue distribution and maintain the drug primarily in the plasma, where it catalyzes the degradation of uric acid.

5. Conclusion

In summary, mPEG-UHC is a new PEGylated mammalian uricase and approximately 9.4 5 kDa mPEG chains were coupled to each UHC subunit based on the determination of average modification degree and PEGylation homogeneity. mPEG-UHC had a specific activity of 12 U/mg and showed significant effect on uric acid nephropathy and acute urate arthritis. After modified with smaller mPEG, the elimination half-live in monkeys is still longer than one week, and the systemic bioavailability of mPEG-UHC after subcutaneous administration is higher than 90%, suggesting that subcutaneous injection may be regarded as a candidate route for administration in clinical trails. Moreover, the non-specific tissue distribution level of mPEG-UHC is lower than other PEGylated uricases. Further chronic toxicity assessments of mPEG-UHC in rodents and non-human primates are currently underway in our laboratory.

Acknowledgements

The research was founded by National Natural Science Foundation of China (20976053/B060804), the Fundamental Research Funds for the Central Universities, Key Project of the National High Technology Research and Development Program of China (2009ZX09306-001) and National Basic Research Program of China (2012CB721100).

References

Baraf, H.S.B., Kim, S., Matsumoto, A.K., Maroli, A.N., 2005. Resolution of tophi with intravenous PEG-uricase in refractory gout. Arthritis Rheum. 50, S105.
Biggers, K., Scheinfeld, N., 2008. Pegloticase, a polyethylene glycol conjugate of uricase for the potential intravenous treatment of gout. Curr. Opin. Investig. Drugs 9, 422–429.
Caliceti, P., Schiavon, O., Veronese, F.M., 1999. Biopharmaceutical properties of uricase conjugated to neutral and amphiphilic polymers. Bioconjug. Chem. 10, 638–646.
Caliceti, P., Schiavon, O., Veronese, F.M., 2001. Immunological properties of uricase conjugated to neutral soluble polymers. Bioconjug. Chem. 12, 515–522.
Chen, R.H., Abuchowski, A., Van Es, T., Palczuk, N.C., Davis, F.F., 1981. Properties of two urate oxidases modified by the covalent attachment of poly(ethylene glycol). Biochim. Biophys. Acta 660, 293–298.
Christen, P., Peacock, W.C., Christen, A.E., Wacker, W.E., 1970. Urate oxidase in primate phylogenesis. Eur. J. Biochem. 12, 3–5.
Coderre, T.J., Wall, P.D., 1988. Ankle joint urate arthritis in rats provides a useful tool for the evaluation of analgesic and anti-arthritic agents. Pharmacol. Biochem. Behav. 29, 461–466.
Conley, T.G., Priest, D.G., 1980. Thermodynamics and stoichiometry of the binding of substrate analogues to uricase. Biochem. J. 187, 727–732.
Edwards 3rd, C.K., 1999. PEGylated recombinant human soluble tumour necrosis factor receptor type I (r-Hu-sTNF-RI): novel high affinity TNF receptor designed for chronic inflammatory diseases. Ann. Rheum. Dis. 58 (Suppl. 1), I73–I81.
Edwards 3rd, C.K., Martin, S.W., Seely, J., Kinstler, O., Buckel, S., Bendele, A.M., Ellen Cosenza, M., Feige, U., Kohno, T., 2003. Design of PEGylated soluble tumor necrosis factor receptor type I (PEG sTNF-RI) for chronic inflammatory diseases. Adv. Drug Deliv. Rev. 55, 1315–1336.
Ekundi-Valentim, E., Santos, K.T., Camargo, E.A., Denadai-Souza, A., Teixeira, S.A., Zanoni, C.I., Grant, A.D., Wallace, J., Muscara, M.N., Costa, S.K., 2010. Differing effects of exogenous and endogenous hydrogen sulphide in carrageenan-induced knee joint synovitis in the rat. Br. J. Pharmacol. 159, 1463–1474.
Fujita, T., Yasuda, Y., Takakura, Y., Hashida, M., Sezaki, H., 1991. Tissue distribution of ^{111}In-labeled uricase conjugated with charged dextrans and polyethylene glycol. J. Pharmacobiodyn. 14, 623–629.
Greenberg, M.L., Hershfield, M.S., 1989. A radiochemical-high-performance liquid chromatographic assay for urate oxidase in human plasma. Anal. Biochem. 176, 290–293.
Hediger, M.A., Johnson, R.J., Miyazaki, H., Endou, H., 2005. Molecular physiology of urate transport. Physiology (Bethesda) 20, 125–133.
Hershfield, M.S., 1998. Adenosine deaminase deficiency: clinical expression, molecular basis, and therapy. Semin. Hematol. 35, 291–298.
Ho, S.N., Hunt, H.D., Horton, R.M., Pullen, J.K., Pease, L.R., 1989. Site-directed mutagenesis by overlap extension using the polymerase chain reaction. Gene 77, 51–59.
Kang, J.S., Deluca, P.P., Lee, K.C., 2009. Emerging PEGylated drugs. Expert Opin. Emerg. Drugs 14, 363–380.
Keebaugh, A.C., Thomas, J.W., 2010. The evolutionary fate of the genes encoding the purine catabolic enzymes in hominoids, birds, and reptiles. Mol. Biol. Evol. 27, 1359–1369.
Kelly, S.J., Delnomdedieu, M., Oliverio, M.I., Williams, L.D., Saifer, M.G., Sherman, M.R., Coffman, T.M., Johnson, G.A., Hershfield, M.S., 2001. Diabetes insipidus in uricase-deficient mice: a model for evaluating therapy with poly(ethylene glycol)-modified uricase. J. Am. Soc. Nephrol. 12, 1001–1009.
Kendrick, B.S., Kerwin, B.A., Chang, B.S., Philo, J.S., 2001. Online size-exclusion high-performance liquid chromatography light scattering and differential refractometry methods to determine degree of polymer conjugation to proteins and protein–protein or protein–ligand association states. Anal. Biochem. 299, 136–146.

Knauf, M.J., Bell, D.P., Hirtzer, P., Luo, Z.P., Young, J.D., Katre, N.V., 1988. Relationship of effective molecular size to systemic clearance in rats of recombinant interleukin-2 chemically modified with water-soluble polymers. J. Biol. Chem. 263, 15064–15070.

Li, X., Zhang, X., Liu, Q., 2005. Determination of the molecular weight distribution of the PEGylated bovine hemoglobin (PEG-bHb). Artif. Cells Blood Substit. Immobil. Biotechnol. 33, 13–25.

Liebman, S.E., Taylor, J.G., Bushinsky, D.A., 2007. Uric acid nephrolithiasis. Curr. Rheumatol. Rep. 9, 251–257.

Liu, Y.P., Li, Q.S., Huang, Y.R., Liu, C.X., 2005. Tissue distribution and excretion of ^{125}I-lidamycin in mice and rats. World J. Gastroenterol. 11, 3281–3284.

Mazzali, M., Hughes, J., Kim, Y.G., Jefferson, J.A., Kang, D.H., Gordon, K.L., Lan, H.Y., Kivlighn, S., Johnson, R.J., 2001. Elevated uric acid increases blood pressure in the rat by a novel crystal-independent mechanism. Hypertension 38, 1101–1106.

Monrad, S.U., Killen, P.D., Anderson, M.R., Bradke, A., Kaplan, M.J., 2008. The role of aldosterone blockade in murine lupus nephritis. Arthritis Res. Ther. 10, R5.

Parkinson, C., Scarlett, J.A., Trainer, P.J., 2003. Pegvisomant in the treatment of acromegaly. Adv. Drug Deliv. Rev. 55, 1303–1314.

Pasut, G., Sergi, M., Veronese, F.M., 2008. Anti-cancer PEG-enzymes: 30 years old, but still a current approach. Adv. Drug Deliv. Rev. 60, 69–78.

Retailleau, P., Colloc'h, N., Vivares, D., Bonnete, F., Castro, B., El Hajji, M., Prange, T., 2005. Urate oxidase from *Aspergillus flavus*: new crystal-packing contacts in relation to the content of the active site. Acta Crystallogr. D: Biol. Crystallogr. 61, 218–229.

Roberts, M.J., Bentley, M.D., Harris, J.M., 2002. Chemistry for peptide and protein PEGylation. Adv. Drug Deliv. Rev. 54, 459–476.

Roth, A., Mollenhauer, J., Wagner, A., Fuhrmann, R., Straub, A., Venbrocks, R.A., Petrow, P., Brauer, R., Schubert, H., Ozegowski, J., Peschel, G., Muller, P.J., Kinne, R.W., 2005. Intra-articular injections of high-molecular-weight hyaluronic acid have biphasic effects on joint inflammation and destruction in rat antigen-induced arthritis. Arthritis Res. Ther. 7, R677–R686.

Safra, N., Ling, G.V., Schaible, R.H., Bannasch, D.L., 2005. Exclusion of urate oxidase as a candidate gene for hyperuricosuria in the Dalmatian dog using an interbreed backcross. J. Hered. 96, 750–754.

Schiavon, O., Caliceti, P., Ferruti, P., Veronese, F.M., 2000. Therapeutic proteins: a comparison of chemical and biological properties of uricase conjugated to linear or branched poly(ethylene glycol) and poly(N-acryloylmorpholine). Farmaco 55, 264–269.

Schlesinger, N., 2004. Management of acute and chronic gouty arthritis: present state-of-the-art. Drugs 64, 2399–2416.

Schlesinger, N., Yasothan, U., Kirkpatrick, P., 2011. Pegloticase. Nat. Rev. Drug Discov. 10, 17–18.

Sherman, M.R., Saifer, M.G., Perez-Ruiz, F., 2008. PEG-uricase in the management of treatment-resistant gout and hyperuricemia. Adv. Drug Deliv. Rev. 60, 59–68.

Stavric, B., Johnson, W.J., Grice, H.C., 1969. Uric acid nephropathy: an experimental model. Proc. Soc. Exp. Biol. Med. 130, 512–516.

Zhang, C., Fan, K., Zhang, W., Zhu, R., Zhang, L., Wei, D., 2012. Structure-based characterization of canine-human chimeric uricases and its evolutionary implications, Biochimie, http://dx.doi.org/10.1016/j.biochi.2012.03.016, in press.